Cleaner Engineering and Technology 26 (2025) 100928

Contents lists available at ScienceDirect

Cleaner Engineering and Technology

journal homepage: www.sciencedirect.com/journal/cleaner-engineering-and-technology

Crude oil production and simulation from catalytic fast pyrolysis of waste polyethylene terephthalate (PET)

E. Avalos-Ortecho [a,*], G. Power-Porto [a], S. Ponce Alvarez [a], M. Gelmi-Candusso [a], C. Pardo-Martinez [b], G. Concha-Oblitas [a]

[a] *Carrera de Ingeniería Industrial, Instituto de Investigación Científica, Universidad de Lima, Peru*
[b] *Universidad del Rosario, School of Administration, Bogotá, Colombia*

ARTICLE INFO

Keywords:
Fast catalytic pyrolysis
Polyethylene terephthalate waste
Crude oil
Zeolite catalyst
Fourier transform infrared spectroscopy (FTIR)
^{13}C nuclear magnetic resonance (^{13}C NMR)

ABSTRACT

Polyethylene terephthalate (PET), a thermoplastic polymer, is the main raw material in the manufacturing of clear bottles used mainly for water and soft drinks. In 2022, the world plastics production was 400.3 million tons; around 6.2 % corresponds to PET, and only 10 % of it is recycled. PET waste can only be recycled four times because high temperatures generate chemical and physical degradation. This study aims to apply the principles of circular economy to transform PET waste into crude oil through fast catalytic pyrolysis, under N_2 atmosphere at different temperatures and with different quantities of zeolite as a catalyst. The crude oil was characterized by Fourier-transform infrared spectroscopy (FTIR) and solution quantitative ^{13}C nuclear magnetic resonance (^{13}C NMR). To compare the test results, a simulation for the pyrolysis reactor was conducted with CHEMCAD software. The result of FTIR analysis showed the presence of carboxylic acids and aliphatic hydroxyl groups, and ^{13}C NMR also shows presence of aromatic C–C and C–O bonds, aliphatic C–O and C–C bonds and carbonyl groups. The experimental results, which were comparable to the simulation, also show that a ratio of 12.5 % zeolite catalyst to waste PET helps the decomposition process and reduces the operating temperature needed in the reactor. There is a positive strong correlation between the reactor temperature and pressure. The highest product yield obtained was 20 % crude oil, 7 % solid powder, 16 % pyrolysis char, and 57 % non-condensable gases.

1. Introduction

Polyethylene terephthalate, or PET, is a thermoplastic used mainly for packaging and to a lesser extent for electrical, electronic, and agricultural applications. In 2022, global production of plastics increased to 400.3 million tons, of which 90.6 % are of fossil origin, 8.9 % are post-consumer recycled plastics and 0.5 % are plastics of biological origin, as shown in Fig. 1. From the global plastic production, 6.2 % corresponds to PET, and China is the main producer with 33 % (Plastics Europe, 2023). After a decrease due to the pandemics, plastics production in the European Union increased to 57.2 million tons in 2021. It is estimated that by 2025 the solid waste generation rate will be 2.25 billion tons (Moya et al., 2017). Plastics currently follow a linear economy (production, consumption, recycling, and final disposal), and poor management generates risks to human health due to GHG emissions (Rosenberg et al., 2021). Consequently, it is essential to change the management of plastic waste from a linear economy to a circular economy (Armenise et al., 2021).

PET waste is difficult to biodegrade and can remain for hundreds of years in the environment (Kubowicz and Booth, 20217), potentially contaminating water and soil with microplastics and, so, affecting biotic resources and people's health (Charlton-Howard et al., 2023). PET recycling has limitations, because every time the waste is recycled it degrades and then becomes waste without the possibility of adding value. Therefore, it is important to find alternatives to recover PET waste applying the principles of circular economy.

Circular economy is a regenerative system in which input resources and waste, emissions and energy loss are minimized by slow closed loops, closures and reduced loss of material and energy. It can also be achieved through long-life design, maintenance, repair, reuse, remanufacturing, renewal, and recycling (Geissdoerfer et al., 2017). On the other hand, Singh et al. (2022) show that the application of biochar to convert waste into byproducts contributes to environmental sustainability and leads to supporting the development of the circular economy. Among the most used technologies are hydrothermal carbonization, gasification, torrefaction, and pyrolysis. Consequently, biochar can also be applied to the conversion of PET waste to fuel through pyrolysis

---

* Corresponding author.
E-mail address: eavalos@ulima.edu.pe (E. Avalos-Ortecho).

https://doi.org/10.1016/j.clet.2025.100928
Received 12 July 2024; Received in revised form 1 March 2025; Accepted 2 March 2025

Abbreviations

BOPP	Biaxially-oriented polypropylene
^{13}C NMR	Quantitative ^{13}C nuclear magnetic resonance
FTIR	Fourier Transform Infrared Spectroscopy
GHG	Greenhouse gas
HDPE	High-density polyethylene
LDPE	Low-density polyethylene
MET BOPP	Metalized BOPP
PE	Polyethylene
PET	Polyethylene terephthalate
PP	Polypropylene
PS	Polystyrene
PVC	Polyvinyl chloride

technology. Likewise, Gracida-Alvarez et al. (2023) says that the application of circular economy for plastics helps reduce material loss and reduces dependence on virgin material. Life cycle and material flow analyses are used to evaluate life cycle analysis and circularity metrics following the implementation of circular economy strategies to produce plastics packaging such as PET bottles. The strategy includes recycling PET bottles and integrating chemical recycling technologies into industrial development such as enzymatic hydrolysis and methanolysis. This strategy reduces the use of virgin material, and greenhouse gas emissions in the value chain from 14 % to 9 % (Ghosh et al., 2023). It also shows that the massive increase in plastic consumption has resulted in uncontrolled plastic pollution both on land and in the sea.

Recovering used plastics can reduce its carbon footprint by displacing virgin plastic production. The strategy consists of creating a network for plastics through a circular economy that includes critical technology, economics and restrictive policies that help decision-making and compare end-of-life options and help investment decisions. Besides, metrics to measure circularity were implemented; the network uses life cycle analysis and compares it with the environmental impact and the route to improve circularity in the plastics economy. Ramos et al. (2023) specify that in the health sector, especially in surgery departments, single-use plastics are used due to convenience in terms of sterility. The results suggest that the design of medical products and packaging does not consider the end of life of the product, making recycling options almost impossible. It is therefore important to consider including waste management hierarchy and end of life in the circular economy (Hossain et al., 2022).

Along the same lines, the plastic waste management system in Australia was studied, analyzing the challenges and opportunities to move towards a circular economy. In terms of polymer types, the most generated (47 % of the total) are LDPE and PET. Most recycling plants use mechanical recycling as the main technological process and market growth was mainly in biodegradable plastics, but lower than expected. Therefore, to improve management, the involvement of all interested parties is needed (Padmanabhan et al., 2022). Energy recovery from used plastics as an alternative fuel source is a sustainable choice and this practice is aligned with that of a circular economy's philosophy. The authors focused on determining the emissions performance standards of fuels from used plastics in a single-cylinder direct injection diesel engine. Erkmen et al. (2023) made a fuel by mixing fuel plastics, 10 % ethane and 10 % ethyl ethoxy acetate as an oxygenated additive to create a quaternary blended fuel. The blended fuel had reduced carbon monoxide emissions. Finally, the pyrolysis process is a thermochemical recycling technology that can be applied to creatively reuse waste plastics and allowing the closure of the gap in the circular economy of plastics.

Pyrolysis is a process of thermal degradation of long chain polymer molecules such as polyethylene terephthalate into short chain molecules. The thermal degradation process is conducted at elevated temperatures and in an inert atmosphere and in the presence of a catalyst to reduce the activation energy of the reactant. The pyrolysis process is a technological alternative to transform PET waste into value-added products such as fuels, oils and thus avoiding the disposal of them in a landfill or another unsuitable place, contaminating the environment (Fulgencio-Medrano et al., 2022). The pyrolysis process to treat used plastics (PVC and PET) rejected from the recycling industry consists of treating the samples with pyrolysis at 460 °C and a residence time of 1 h, obtaining the highest liquid yield (70.6 % at 460 °C). The effect of temperature in the range of 430–490 °C was also investigated. Used plastics were processed into fuels using a pyrolysis reactor and ZSM-5 zeolite catalyst (both commercial and synthesized) and compared with other catalysts. The results show that the ZSM-5 zeolite was more effective using the hydrothermal technique with metakaolin as a source of alumina. The authors used a mixture of plastics (BOPP, MET BOPP, PET) in the presence of more than one catalyst with an average loading of 2 kg. Waste biaxially oriented polypropylene (BOPP) plastics had a higher performance in terms of heat and fuel compared to used PET

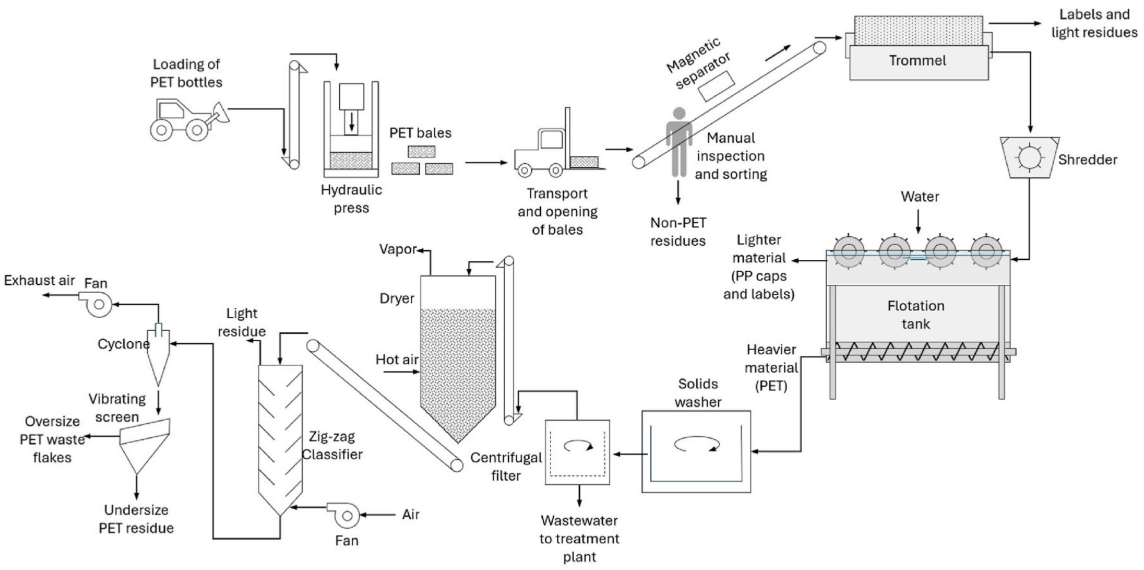

Fig. 1. Process flow diagram of the production of waste PET flakes.

plastics. The synthesized ZSM-5 zeolite produced a maximum fuel efficiency of around 70 % and a corresponding gas and carbon (particles) of 16 % and 14 %, respectively, for low-density polyethylene (Sivagami et al., 2022a). Other researchers have also shown the fast catalytic pyrolysis process as an alternative for processing PET waste (Jia et al., 2020; Papuga et al., 2022).

Catalysts play a significant role in the pyrolysis process with the aim of degrading PET waste and obtaining fuels with better performance. The reduction in activation energy achieved by the catalyst allows a reduction in processing time. Yansaneh and Zein (2022) processed polyethylene, polyethylene terephthalate, polystyrene by catalytic pyrolysis. Their results show that in the temperature range of 390 °C and 425 °C with the use of a catalyst the activation energy of the reaction is reduced and fuels with better performance are produced. Zeolite, silica-alumina, $CaCO_3$, $MgCO_3$, among others, were used as catalysts. For the pyrolysis of PET, Al-(Al_2O_3) was used as a catalyst at a temperature range of 250–500 °C and a duration between 20 and 90 min. The products obtained were benzene, styrene, meta ethylstyrene, biphenyl and naphthalene. On the other hand, Sivagami et al. (2022) used ZSM-5 zeolite as a catalyst; they made a comparison of the performance of ZSM-5 and the ZSM-5 synthesized in the laboratory for the pyrolysis process of plastics. In the case of PET, the temperature was kept in the range of 450–500 °C, obtaining a product of 10 % oil, 42 % gases and 48 % carbonized material. Also, Eimontas et al. (2021) used ZSM-5 as a catalyst in different proportions with respect to the waste plastics (0 %, 10 %, 30 % and 50 %); their results show that at 50 % ZSM-5 a better performance was achieved, and the fuel was composed of volatile and flammable components (benzene, toluene, and hexane) (Li et al., 2021). They processed PET in a bed reactor over a zeolite catalyst, obtaining solid, liquid, and gaseous fuels as products at a reaction temperature of 500 °C.

The results show that zeolite has a significant influence on the primary and secondary reactions; also, the content of olefins such as C (59.8 %), H (4.8 %), O (35.4 %) and C/H ratio of 1.0 were determined by analysis. Regarding the specific area and porous structure of the catalyst, a pore volume of 0.17 and 0.12 cm^3/g and a surface area of 13.2 and 6.6 m^2/g, before and after the reaction, respectively, were found. Miandad et al. (2019) processed various used plastics (PS, PE, PP and PET) by catalytic pyrolysis using zeolite (activated with HNO_3 at 550 °C) as a catalyst in different proportions in a pilot-scale reactor. The products obtained were analyzed by chromatography and mass spectrometry, finding mixtures of aromatic and aliphatic compounds, as well as other hydrocarbons. Finally, Jia et al. (2020) processed PET by fast catalytic pyrolysis using ZSM-5 zeolite and nickel chloride as catalysts at different temperatures (450 °C–600 °C) and inert conditions (nitrogen flowrate 200 mL/min). The proportion of aromatic hydroxyl groups increased to 21.82 % when the mass ratio of zeolite to PET was 2.0; the result shows that the ZSM-5 catalyst can facilitate the decomposition of aliphatic and carboxylic groups.

According to (LePree, 2015)"modeling and simulation software are not only very powerful but also because of their user-friendly nature, being a very valuable tool in chemical processes that use different types of simulation packages to optimize equipment, processes, and good practices. An advanced use of process simulation software is in operations where simulators are often used to compare current performance against new process designs". On the other hand, Krzywda and Wrzesińska (2021) say that the design of the condensation and fractionation unit affects the quantity and quality of the liquid products derived from the pyrolysis of plastic waste; the products obtained qualify as a fuel alternative. For the simulation, they used the CHEMCAD software and found that the conversion and oil fractions practically do not depend on the temperature of the feed stream. To simulate a process with CHEMCAD it is particularly important to be exact with the calculations of properties such as enthalpy, entropy, and fugacity (James et al., 2020; Andersen et al., 2018). They simulated the pyrolysis process from plastic waste, obtaining results close to those obtained in pilot tests. Mabitsela et al. (2022) also simulated and optimized the production of nitric acid with CHEMCAD version 7.0. On the other hand, Potnuri et al. (2022) modeled and optimized biomass and used plastics using CHEMCAD, Matlab, Machine Learning, Aspen, among other software packages.

Considering that previous studies of fast catalytic pyrolysis of PET waste have been oriented towards the evaluation of parameters, such as temperature, heating rate and different types of PET waste, and their effect on the performance of the fuel obtained, there are few studies regarding the effect of the zeolite catalyst, when the ratio of this catalyst is modified and the effect on the yield of the crude oil obtained, as well as the effect of modifying the temperature in the catalytic pyrolysis process in a fixed bed reactor. On the other hand, there are few studies on the simulation of obtaining crude fuel from PET waste using software and comparing the results with laboratory-scale catalytic pyrolysis tests. Therefore, the present work aims to find the effect on the performance and composition of the raw fuel obtained by fast catalytic pyrolysis with the variation of the amount of zeolite catalyst and temperature, determined by simulation with CHEMCAD software version 8.1. The crude oil obtained through a mass and energy balance for the pyrolysis process is compared with the tests obtained on a laboratory scale. On the other hand, the results obtained in bulk will be represented in a Sankey diagram, relating the amount of PET waste and the products obtained. Besides, FTIR analysis will be performed to determine the presence of functional groups in the crude fuel and quantitative nuclear magnetic resonance (^{13}C NMR) analyzes to determine the composition of the crude oil. The question of this research is: What effect does the variation of catalyst weight and temperature have on the yield and composition of crude oil obtained from PET waste through fast catalytic pyrolysis? This article is structured in five sections: introduction, materials and methods, results and discussion, and conclusion, that was made possible by this study.

2. Materials and methods

Before being treated in the pyrolysis unit, waste PET bottles must be physically conditioned through a series of unit operations. On the other hand, zeolite must be activated at elevated temperatures in a benchtop tubular muffle furnace under inert atmosphere conditions, so that it can be later used as an activated catalyst in the fixed bed reactor.

2.1. Materials

Waste PET bottles were physically conditioned in the Gexim SAC waste PET processing plant; unit operations included pressing, classification, grinding, washing, drying, and screening. The process flow diagram of this plant is presented in Fig. 1. The waste PET flakes were classified using a screen to obtain a homogeneous particle size of 4.5 mm. The 10 kg waste PET flake sample was selected randomly. The sample of waste PET flakes was heated in an oven up to 110 °C for 24 h with the aim of removing residual moisture. Subsequently, the sample was stored in a desiccator with the aim of avoiding absorption of humidity from the environment and contamination problems. A characterization of the PET was performed. Artetxe et al. (2010) and Grause et al. (2011) show results like those in Table 1a. The composition of C, H and O of the sample was 61.87 % by weight, 4.35 % and 33.78 %, respectively, and similar to the values of virgin PET (C, 62.5 %; H, 4.2 %; O, 33.3 %). There is also an agreement with Du et al. (2016). Kumagai

Table 1a
Analysis of waste PET flakes.

Proximate Analysis	Volatile matter	Fixed Carbon	Ash
Wt.% dry basis	88.54	9.37	2.09
Ultimate analysis	**C**	**H**	O[a]
Wt.% dry basis	61.87	4.37	33.78

[a] By difference, according to Jia et al. (2020).

Table 1b
BET analysis results of zeolite.

Characteristic	Value
BET surface area	17.9613 +/− 0.0341 m^2/g
Slope	5.38024 +/− 0.01022 g/mmol
Correlation coefficient	0.9999874
Molecular cross-sectional area	0.1620 nm^2

et al. (2015) also found comparable results to the indicated conditions. The analyses of waste PET flakes are shown in Table 1, below (Jia et al., 2020).

2.1.1. Activation and characterization of the zeolite catalyst

The zeolite raw material, which is dark green in color, was bought from Química Industrial in Lima, Peru. To activate the zeolite, it was placed in a tubular muffle furnace at 550 °C for a period of 6 h with an inert atmosphere (gaseous nitrogen is injected). The muffle has a THOZ temperature controller. Six crucibles with zeolite inside a quartz tube, with an average weight of 10 g each, are fed to the muffle with the objective of removing contaminants and humidity. To insulate the muffle and prevent heat loss, mineral wool is placed around the muffle and sealed. The clamping flanges are then connected to hold the quartz tube at the ends of the muffle; then, the temperature controller is programmed so that the temperature increases an average of 10 °C/min until it reaches 550 °C. After 50 min, at 550 °C, the program is turned off, so that the temperature remains constant for the remaining time, until 6 h have passed.

After 6 h, the heater is shut off and the muffle cools down for an hour. Next, the crucibles with the activated zeolite are removed. The color changed from dark green to a khaki yellow. The activated zeolite is placed in metalized plastic bags and stored in a desiccator until it is needed in the pyrolysis process.

After the zeolite was activated, the surface area was determined by the Brunauer-Emmett-Teller (BET) method in the Environmental Engineering Laboratory of University of Lima (the same procedure was followed by Muneer et al. (2019). The equipment used was a Micromeritics Instrument Corp. Gemini VII version 5.03, with nitrogen adsorption at a temperature of 25 °C. The results are shown in Table 1b.

2.2. Experimental procedure

The PET flakes were processed in the fixed-bed fast catalytic pyrolysis unit on a laboratory scale under inert conditions by feeding gaseous nitrogen, according to Sharuddin et al. (2017). The PET waste sample was placed in the lower part of the fixed-bed reactor (168 mm inner diameter × 290 mm height and 5 L internal capacity). On top of that load the activated zeolite catalyst was added. After feeding the charge to the reactor, the reactor cover was placed and sealed, tightening the eight bolts with a torque of 110 N-m. Next, gaseous nitrogen was fed at a flow rate of 4.5 L/min for 15 min while keeping the reactor valve open. The goal of this is to eliminate all the oxygen from the reactor vessel. Then, the reactor valve was closed, and the process continued, feeding N_2 to support an inert atmosphere until the pressure in the nitrogen tank valve began to decrease (this happened after approximately 30 min); at that moment, the N_2 feed valve was closed. The internal temperature in the fixed-bed pyrolysis reactor was measured with a thermocouple connected to the real-time temperature controller.

As shown in Figs. 2 and 3 and Table 2, the pyrolysis unit consists of the reactor chamber, electrical heating jacket with thermal insulation, manometer to control the pressure in the reactor, condenser for the pyrolysis gasses, condensate holding tank, chiller with glycol refrigerant (condenser inlet temperature between 0 °C and −5 °C), and pressurized nitrogen tank with pressure and flow controls. Besides, a 220-VAC 3-phase power supply unit is provided with a PLC control panel for recording variables such as temperature and pressure inside the reactor, nitrogen flow rate, reaction time, temperature of pyrolysis gasses, and refrigerant entering the condenser. The whole pyrolysis unit was hermetically enclosed within tempered glass walls; on top of this enclosure, a stainless-steel hood and an exhaust system with activated carbon adsorption filter was provided to eliminate odors and potentially toxic gasses; then the treated gasses were vented to the atmosphere. Fig. 6 shows a detailed scheme of the pyrolysis unit.

The heating rate in the reactor was 10 °C/min on average, according to the parameters required for fast pyrolysis. The amount of catalyst was either 0, 100 or 200 g, to evaluate the effect on the performance of the pyrolysis condensate product, referred to as crude oil, while the PET flakes grain size was kept at 4.5 mm (Anuar Sharuddin et al., 2017). The average duration of each test run was 60 min, with temperatures of 380 °C, 430 °C and 480 °C, as shown on Table 3. The pyrolysis gasses generated by the thermochemical decomposition of the PET flakes meet the catalyst and rise under pressure through the upper part of the reactor and condense by heat exchange with the refrigerant that enters the condenser in countercurrent between −3 °C and 0 °C. Particulate matter entrained in the gasses are also deposited in the pipes and condenser, while the crude oil condensate with a waxy appearance is received in the holding tank.

According to Montgomery (2017), it is valid to carry out a single replication of 2^k factorial design experiments (non-replicated factorial design) and it is used when the available resources only allow a single replication of the design, and the factors to be evaluated are a relatively large number. Likewise, Daniel (1959) suggests examining a normal probability graph of the estimates of the effects, the effects that are insignificant follow a normal distribution, with zero mean and variance σ^2, and will tend to be located on a straight line in the graph, while the significant effects will have means different from zero and will not be located on the straight line. In this case, the factors that have a significant effect on the performance of the raw fuel are the temperature and the catalyst.

When the condensate tank valve is opened, the non-condensable gases come out first and are vented through the exhaust system. Then, the khaki-colored crude oil is discharged into a 200-mL heat-resistant borosilicate flask and the volume was measured. After about 10 min, two phases are formed in the flask: at the bottom, pyrolysis particles (solid powder), and in the upper phase the supernatant crude oil. The pyrolysis particles are separated from the crude oil by centrifugation and then weighed, the pyrolysis carbon is removed from the reactor and weighed. The weight of the crude oil was calculated by multiplying the volume by its density (0.9673 g/cm^3). In total, eight tests were conducted, two of them were discarded due to operational problems (pyrolysis gas leaks through the reactor lid and the reactor bottom plug). Details of the tests are presented in Table 3. From each test the following products were obtained: pyrolysis carbon, crude oil (plus particulate matter from the pyrolysis process), and non-condensable gasses. To find the amount of non-condensable gasses, a material balance is formulated according to equation (1); the yield of crude oil in weight percentage is calculated with equation (2).

$$W_{\text{non-condensable gases}} = \left(W_{\text{sample}} + W_{\text{catalyst}}\right) - \left(W_{\text{crude oil}} - W_{\text{char}} - W_{\text{solid powder}} + W_{\text{catalyst}}\right. \tag{1}$$

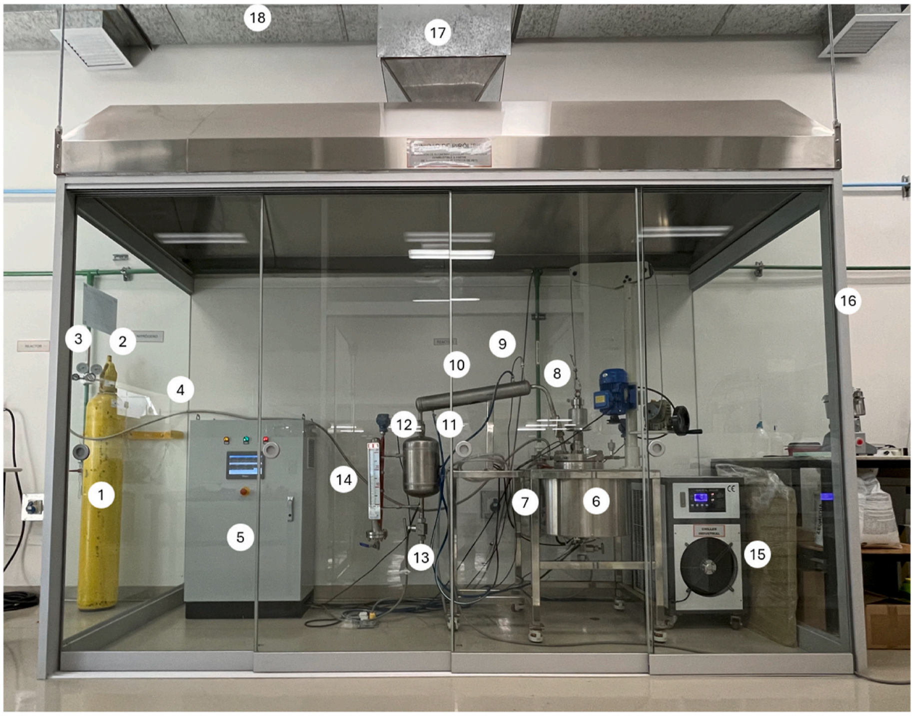

Fig. 2. Laboratory-scale fast catalytic pyrolysis unit with hermetic insulation and fugitive emissions treatment system.

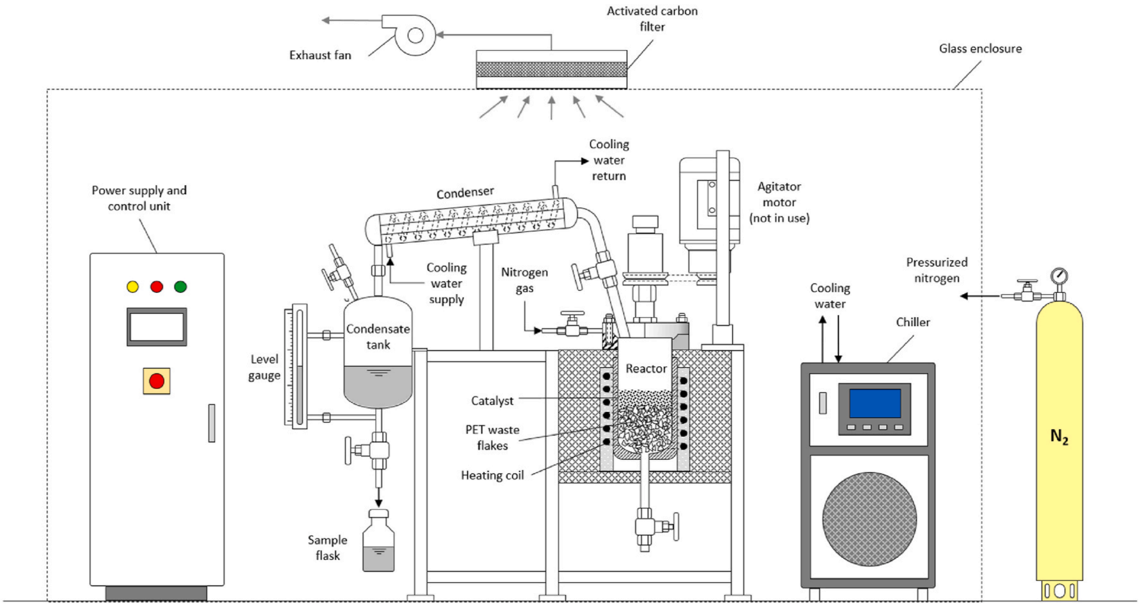

Fig. 3. Detailed scheme of laboratory-scale fast catalytic pyrolysis unit.

Table 2
Legend for laboratory scale fast catalytic pyrolysis unit.

No.	Equipment	No.	Equipment
1	Nitrogen gas tank	10	Condenser
2	Nitrogen control valve	11	Cooling hose
3	Nitrogen flow meter	12	Crude oil tank
4	Metal-braided nitrogen hose	13	Condensate control valve
5	Process variables control panel	14	Condensate tank level gauge
6	Fixed bed pyrolysis reactor	15	Chiller unit
7	Reactor jacket	16	Glass enclosure
8	Thermocouple for the reactor	17	Activated carbon filter
9	Thermocouple for pyrolysis gasses	18	Treated gas ventilation system

Table 3
Summary of pyrolysis test data.

Sample	Weight (g)	Catalyst (g)	Temperature (°C)	Duration (min)	Nitrogen (L/min)
M1	800	100	380	60	4.5
M2	800	200	430	60	4.5
M3	800	0	480	60	4.5
M4	800	100	430	60	4.5
M5	800	200	480	60	4.5
M6	800	0	380	60	4.5

$$Yield_{\text{crude oil}} = \left(W_{\text{crude oil}} \;/\; W_{\text{PET flakes}}\right) \times 100\ (\%) \tag{2}$$

The sample weight (W_{sample}) was 800 g for each test, and the weight of catalyst (W_{catalyst}) was 0, 100 or 200 g, according to Table 3.

2.3. Characterization of spent PET flakes, PET bottles, zeolite, and crude oil from pyrolysis by FTIR

After the fast catalytic pyrolysis process, the following products are obtained: pyrolysis carbon, inside the pyrolysis reactor, crude oil, solid powder, and non-condensable gases. Used PET flakes, PET bottles, zeolite and pyrolysis products were analyzed in the Environmental Engineering laboratory of the University of Lima. The crude oil analyses were conducted with a Fourier-transform infrared spectrophotometer Shimadzu, IRTracer100 equipment. Analysis conditions were temperature 20 °C, 45 % relative humidity, FTIR spectra range of 4000 to 400 cm^{-1}.

2.4. Analysis of the crude oil by ^{13}C NMR

After processing the 6 samples of waste PET flakes at different concentrations of zeolite catalyst and different temperature ranges in the laboratory-scale catalytic pyrolysis unit, the waxy products obtained were characterized using a Bruker Fourier 300 HD 300 MHz spectrometer. 50 mg of samples were weighed and dissolved in 1.5 mL of dimethyl sulfoxide (DMSO-d6). The experiments were ^{13}C NMR. The number of scans was 1024, with a pulse delay of 5 s (Ben and Ragauskas, 2011; Kosa et al., 2011). The analyses were conducted at room temperature. The spectral signals were adjusted with the solvent signal (39.52 ppm.) The processing of the spectra was conducted using the TopSpin 3.2 software from Bruker. The analyses were conducted in the laboratory of the Institute of Chemistry of the Faculty of Science of the Pontifical University of Valparaiso, Chile.

2.5. Fast catalytic pyrolysis simulation with CHEMCAD

A typical simulation in CHEMCAD follows the following steps: Start a new simulation, specify engineering units, select chemical components, select-K value and enthalpy, draw the flowsheet, define the feed streams, enter specifications for the unit operations, run the simulation and review the results of simulation.

However, before the simulation can be carried out, it is necessary to gather all the available data of unknown substances, in this case PET, so it can be defined and entered in the component database of the CHEMCAD software. The first step is to decide the average polymer formula, based on its average molar mass.

In a polymer, the ends of the chain are completed with the initiator and terminator radicals, respectively, and their chemical composition essentially doesn't change the average composition of the polymer, so their contribution to the molar mass is also negligible. The chemical formula is $[C_{10}H_8O_4]_n$, where n represents the average degree of polymerization, which can be estimated from the polymer's molar mass of 10–50 kg/mol. The actual value depends on the actual degree of polymerization according to the application; for instance, 20 kg/mol for textile-grade PET, and 37 kg/mol for bottle-grade PET. The next step consists in compiling physical and thermodynamic properties to be entered in the CHEMCAD simulation software. Table 4 shows the collected data and sources.

Table 4

Compiled physical and thermodynamic properties of PET (CAS # 25038-59-9).

Property	Symbol	Value	Unit	Sources
Average molar mass	M_n	21 700–37 000	g/mol	Farah et al. (2015)
		25 038	g/mol	ChemBk
		10–50	kg/mol	Wikipedia
Density	ρ	1.33–1.48	g/cm^3	Polymer Database
		1.370–1.455		Wikipedia
		1.10–1.20		MatWeb
Melting point	T_m	250–265	°C	ChemBk, Wikipedia
Boiling point	T_b	>350 (decomposes)	°C	Wikipedia
Intrinsic viscosity	η	0.55–0.75	dL/g	Farah et al. (2015)
Kinematic viscosity (liquid)	η	250–400	Pa·s	ChemBk
Enthalpy of melting (Latent heat of melting)	$\Delta_m H$	26.9 56.2 powder 140.1 crystalline	kJ/mol kJ/kg kJ/kg	Blaine (n.d.) Gu et al. (2019) Setaram (2020)
Higher heating value	HHV	30.2	MJ/kg	Papari et al. (2021)
Lower heating value	LHV	24.3 ± 0.13	MJ/kg	Lyon et al. (1998)
Standard formation enthalpy (Heat of formation)	$\Delta_f H$	−270.52	kJ/mol	The Polymer Design Team (2016)
Specific heat capacity	c_P	1030 (solid)	J/(kg·°C)	The Engineering Toolbox
		219.3 (solid)	J/(mol·K)	Polymer Database
		303.4 (liquid)	J/(mol·K)	

1from the magnitude of the value, it can be inferred that mole stands for one monomer unit.

2.5.1. Degree of polymerization

Due to the thermal degradation of the polymer during processing and recycling, a mean value of 30 kg/mol is considered, and the degree of polymerization (n) has been calculated as follows equation (3):

Molar mass (g/mol):

$$C = 12.011;\ H = 1.00784;\ O = 15.999;\ C_{10}H_8O_4\ (\text{monomer}) = 192.17$$

$$n = 30\,000 \;/\; 192.17 = 156.11 \approx 156 \tag{3}$$

For the indicated range of 10–50 kg/mol, the degree of polymerization corresponds between 52 and 260.

2.5.2. Standard enthalpy of formation

The two values of heating value (enthalpy of combustion) coincide, because they only differ in the latent heat of condensation of water. The combustion reaction can be written as follows equation (4):

$$C_{10}H_8O_4\ (s) + 10\ O_2\ (g) \rightarrow 10\ CO_2\ (g) + 4\ H_2O\ (g) \tag{4}$$

Stoichiometrically, 10 mol of CO_2 and 4 mol of H_2O per each mole of PET (monomer) are generated; this equates to 10 × 44.01/192.17 = 2.2902 kg CO_2/kg PET, and 4 × 18.02/192.17 = 0.3751 kg H_2O/kg PET. equation (5) below is used to calculate the standard enthalpy of formation from the lower heating value:

$$-24300\ \text{kJ}\,/\,\text{kg} = 2.2902(-393.51\ \text{kJ}\,/\,\text{mol}\ \ /\ \ 0.04401\ \text{kg}\,/\,\text{mol}) + 0,3751(-241.83\ \text{kJ}\,/\,\text{mol}\ \ /\ \ 0.01802\ \text{kg}\,/\,\text{mol}) - \Delta_f H_{\text{PET}} - 0 \tag{5}$$

In the previous equation, the last value is the enthalpy of formation of oxygen, which is zero, by definition (pure substances). The standard enthalpy of formation of PET results in a value of −1211.4 kJ/kg, equivalent to −36,3 MJ/mol for a polymerization grade of 156 (with the value of −270.52 kJ/mol for the monomer from Table 4, a polymerization grade of 134 is deduced).

2.5.3. Vapor pressure

For vapor-liquid equilibrium (VLE), vapor pressure as a function of temperature is necessary. In this case, published data from diverse types of plastics were used (Jensen, 1956). The closest material in composition was polyethylene, whose vapor pressure is given by equation (6):

$$\log P = 7{,}4\text{–}4500/T \ [\text{mm Hg}] \qquad (6)$$

However, CHEMCAD uses vapor pressure in Pascals (Pa) with the following exponential equation:

$$P = \exp(A + B / T) \qquad (7)$$

Converting the coefficients, values of A = 21.93187 and B = −10361.63 were obtained. As an example, the vapor pressure at 25 °C (298.15 K) is 2.68 × 10^{-6} Pa (2.01 × 10^{-8} mm Hg).

3. Results and discussion

The results are shown below according to the 6 tests conducted as indicated in Table 3.

3.1. Characterization of the zeolite catalyst

In Fig. 4, the wavelength patterns for the zeolite (FTIR) are shown; the wavelength of 1020 cm^{-1} corresponds to silicon oxide (SiO_2). Table 5a shows the composition of zeolite according to the manufacturer's information.

3.2. Characterization of PET flakes and PET bottles

The functional groups of PET flakes and bottles according to the FTIR analysis are shown in Fig. 5 and Table 5b. According to Artetxe et al. (2010), and Du et al. (2016), random bond breaking of ester bonds leads to the formation of carboxylic and vinyl ester functional groups, when PET is heated to higher temperatures of 385 °C (Dhahak et al., 2019). Likewise, some small molecular bonds including acetaldehydes, CO_2, CO and ethylene are formed due to the instability of vinyl ester (Çit et al., 2010; Venkatachalam et al., 2012).

Table 5a
Zeolite composition according to manufacturer's information.

Component	Wt. %
SiO_2	97.76
Al_2O_3	1.97
Na_2O	0.17

3.3. Performance of crude oil from pyrolysis with and without zeolite catalyst

Fig. 6 shows the results obtained in percentage yield from the processing of PET waste flakes in the fast catalytic pyrolysis process unit. The six tests were conducted varying the temperature between 380 °C, 430 °C and 480 °C and dosing the amount of the zeolite catalyst between 0 %, 12.5 % and 25 % ($W_{\text{catalyst}}/W_{\text{PET}} \times 100$). The residence time was 60 min for each of the tests, gaseous nitrogen was fed at a flowrate of 4.5 L/min and the PET waste flakes were sieved to a size of 4.5 mm, with a sample weight of 800 g for each batch. The results show that in the absence of catalyst (sample M3, 480 °C) the greater amount of crude oil (66 %) is generated (compared to sample M6, 380 °C, 58 %), according to Lee (2012). In this case it is because thermal pyrolysis, as an endothermic process, produces long chain compounds (López et al., 2011) and the crude oil is of low quality due to the low octane number and the presence of high levels of solid residues (Kim and Kim, 2004). On the other hand, the zeolite catalyst influences the composition of the pyrolysis products, and as it is seen that at the same temperature (430 °C) the increase of the catalyst from 12.5 % (M4) to 25 % (M2). It is verified that the greater the amount of catalyst, the greater number of generated gases (M4, 58 %, M2, 71 %), and the lesser production of crude oil (M4, 20 %, M2,12 %); however, the composition of the compounds improves in said product (Du et al., 2016). On the other hand, Diaz-Silvarrey et al. (2018) used ZSM-5 as a catalyst for the processing of PET waste and the gas yield increased from 38.19 % to 55.91 %, that is, there was an increase of 29 % at the temperature of 600 °C with a catalyst/PET ratio from 0 % up to 10 % by weight. In this research, when no catalyst was used at a temperature of 480 °C, the gas yield is 18 % in M3, but when the catalyst concentration was increased to 25 % and at a temperature of 480 °C, a yield of 63 % was achieved, that is, there is an increase of 60.3 % of gases due to the greater breakage of the C–C bonds facilitated by the greater amount of catalyst; therefore, the trend towards the increase in gases is similar. The same trend is also observed in the results of Jia et al. (2020), without catalyst at a temperature of 450 °C a gas yield of 19 % was obtained, while when the ratio catalyst/PET is from 6/1 the gas yield increases up to 69 %.

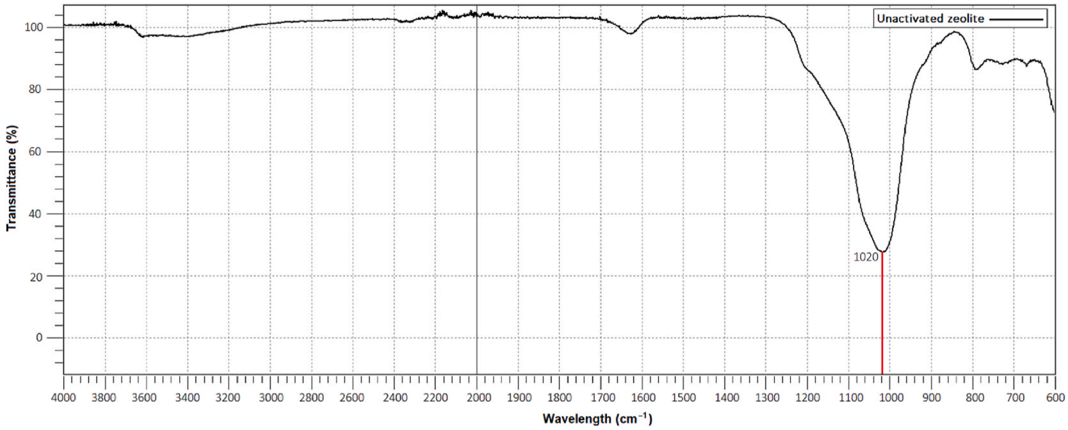

Fig. 4. Wavelength patterns (cm^{-1}) for zeolite by FTIR.

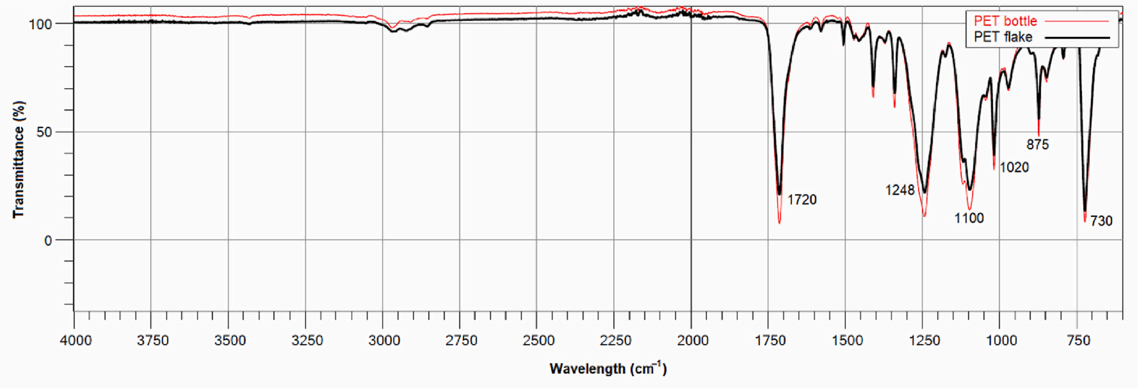

Fig. 5. Wavelength patterns for used PET flakes and PET bottles.

Table 5b
Functional groups of PET flakes and bottles according to FTIR.

Wavenumber, cm^{-1}	Bond	Functional group
1720	C=O	Aldehydes
1248, 1100, 1020	CO	Alcohols, esters, ethers, carboxylic acids, acid, anhydrides
875, 730	CH (out of plane bend)	Aromatics

3.4. *Correlation between the temperature and pressure variables in the pyrolysis process*

According to the observations in the rapid catalytic pyrolysis process of waste PET flakes, it is important to evaluate the correlation trend existing between the input variables and the output responses (Zhang et al., 2020a, 2020b, 2021, 2022, 2024). Fig. 7 shows the trend in pressure as a function of temperature, at intervals of 5 min throughout the process that lasted an average of 60 min. In all the tests conducted, the heating in the reactor was done by heat transfer through the jacket around the reactor. On average, during the first 35 min of the pyrolysis process, only nitrogen is injected to generate an inert atmosphere inside the reactor and thus to prevent the waste PET flakes from being consumed due to the heat. Likewise, Table 6 shows the coefficients of determination, Pearson, and correlation for samples M1, M4 and M5 for temperature (independent variable) and pressure (dependent variable), like those of Maafa (2021). According to Fig. 6, for M1, M4 and M5 together, temperature and pressure have a strong positive correlation: 0.8423, 0.8998 and 0.8411 for each of the samples, respectively; however, it is observed that the best correlation is for M4 (0.8998) where the pyrolysis process was carried out at a temperature of 430 °C, which would generate a greater yield of the crude oil. Regarding the Pearson coefficient, a positive correlation of 0.8423, 0.8883 and 0.8412 is also observed for each of the samples M1, M4 and M5 respectively, observing that there is a strong correlation in M4, which would indicate that at 430 °C a better performance in the pyrolysis product and a better composition of the functional groups that make up the crude oil would be achieved. This finding is remarkably like the study by Vaishnavi et al. (2023), who found a value of 0.857 as a Pearson coefficient for the plastic pyrolysis process. Similarly, the same trend is seen for the coefficient of determination, where the highest value is 0.8096 for M4, which is interpreted as 80.96 % of the pyrolysis pressure values are explained by the independent variable temperature; These results are consistent with the findings of Lombardo et al. (2021).

Likewise, it is observed in Fig. 7 that at 350 °C in each of the samples M1, M4 and M5, the pressure in the fixed bed reactor increases, the pressures at these temperatures are 0.31, 0.54 and 0.31 MPa

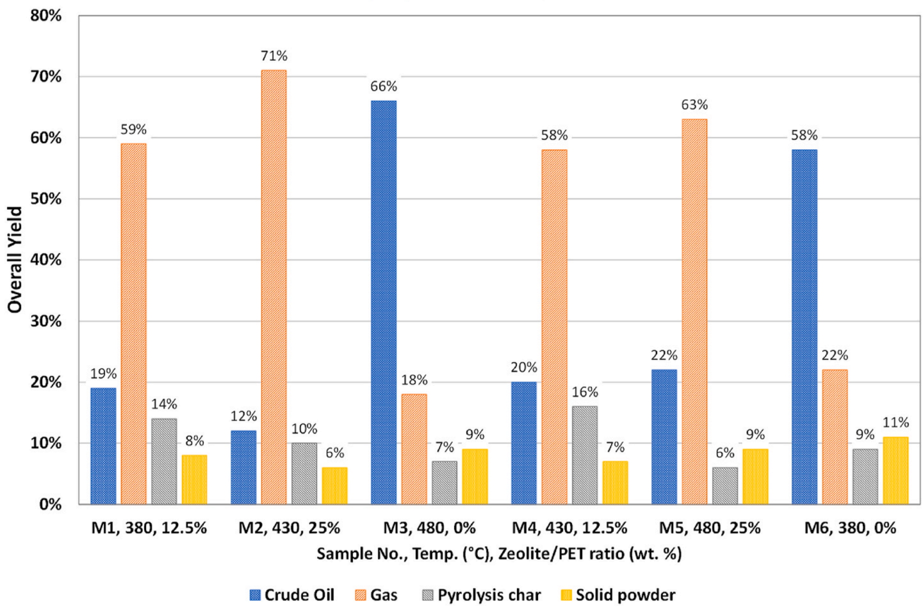

Fig. 6. Effect of temperature and catalyst on total crude oil yield.

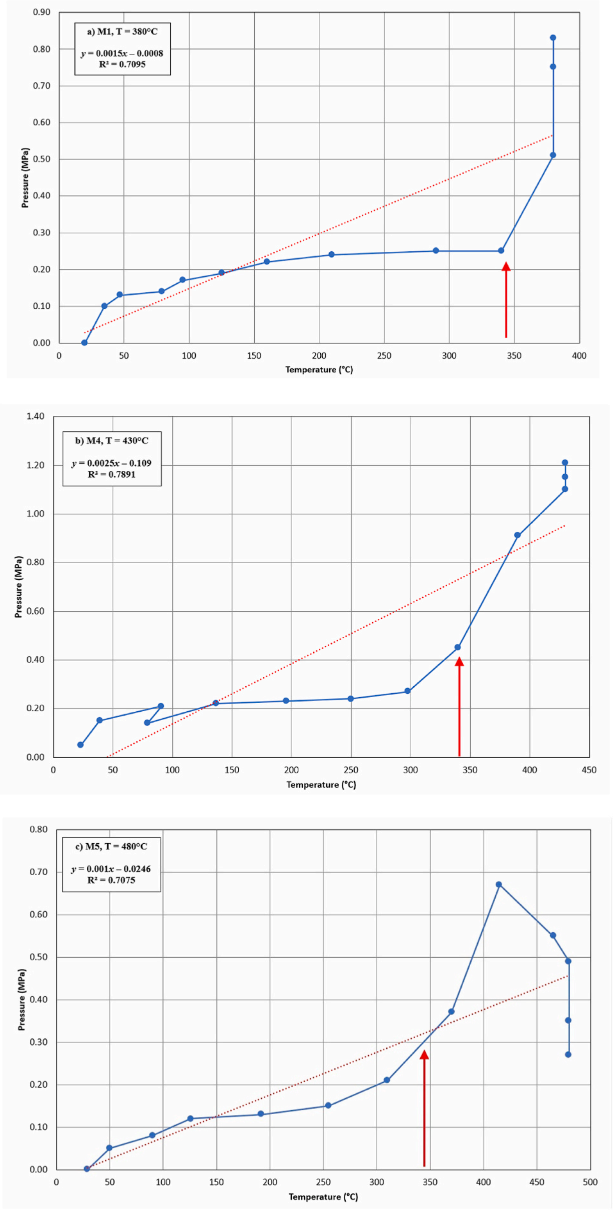

Fig. 7. Trend between temperature and pressure of the fast catalytic pyrolysis process of waste PET flakes for samples M1, M4 and M5.

Table 6
Coefficient of determination, Pearson, and correlation at temperatures of 380 °C, 430 °C and 480 °C.

Sample	Temperature	Determination coefficient	Pearson coefficient	Correlation coefficient
M1	380	0.7095	0.8423	0.8423
M4	430	0.8096	0.8883	0.8998
M5	480	0.7075	0.8412	0.8411

respectively in a time of 46.25, 41 and 33.33 min respectively and a maximum pressure of 0.81 MPa is reached in each of the samples at 55 min in M1, 1.21 MPa at 55 min in M4 and 0.67 MPa at 40 min in M5. According to these results, it is inferred that, at 350 °C, the generation of pyrolysis gases begins due to the increase in pressure in the reactor because of the breaking of C–C bonds and on average 50 min after starting the pyrolysis process, the maximum pressure which indicates that it is the moment where the greatest amount of crude oil is produced. On the other hand, given that the maximum pressure of 1.21 MPa is reached in M4, it is concluded that a better crude oil yield would be obtained at 430 °C. These results have a certain degree similarity with the findings of Yansaneh and Zein (2022), who conducted tests in the range of 390–425 °C, obtaining an oil with better performance.

3.5. *Effect of zeolite catalyst on crude oil composition*

As indicated in the methodology, 800 g of waste PET flakes are fed to the reactor and the zeolite catalyst is then placed on the PET flakes, with the aim that after heating under inert conditions by injection of nitrogen, the PET is sublimed, and the pyrolysis gases meet the catalyst layer and thus reduce the activation energy of the endothermic reaction required for the decomposition of the PET. In the tests carried out, the effect of the catalyst on the composition of the crude oil was evaluated in a range of mass percentage of catalyst/PET flakes waste of 0 %, 12.5 % and 25 %, at temperatures of 380 °C, 430 °C and 480 °C and feeding a nitrogen gas flow of 4.5 L/min (Jia et al., 2020).

3.5.1. *Analysis of crude oil composition by FTIR*

Fig. 8 presents the FTIR analysis for the crude oil at temperatures of 380 °C, 430 °C and 480 °C, with zeolite catalyst (100 and 200 g) and without catalyst, for a feed by load of waste PET flakes. 800 g (catalyst/PET flake waste ratio; 12.5 % and 25 %), supplying the fluidized bed pyrolysis reactor with a nitrogen flow of 4.5 Lit/min to generate an inert atmosphere inside the reactor. Considering the infrared spectrum of the 6 tests carried out, it is observed that temperature does not have a significant effect, according to the ranges analyzed (temperatures evaluated were 380 °C, 430 °C and 480 °C) on the composition of the functional groups, which coincides with the findings of Diaz- Silvarrey et al. (2018). The spectra in general show the presence of olefin functional groups and carbonyl groups. Phenols and alcohols (OH), CH bonds and CN bonds, which are found at 3425, 940, 710, 1310-1340 cm^{-1}, respectively (Nait-Ali et al., 2011; Olcese et al., n.d.). Likewise, two small peaks are identified at 2995, 1699 cm^{-1}, which indicates the presence of stretch CH in alkenes, and C=O bonds that correspond to carboxylic acids, these findings have some similarity with Dhahak et al. (2019). On the other hand, two more pronounced peaks are observed at 1157 and 1090 cm^{-1}, with CO bonds that show the presence of alcohols, esters, ethers, and carboxylic acids. All these findings of the functional groups found by the FTIR analyzes also coincide with the findings of Jia et al. (2020).

3.5.2. *Crude oil analysis by quantitative ^{13}C NMR*

A characterization of the crude pyrolysis oil was conducted using quantitative nuclear magnetic resonance ^{13}C NMR with the aim of visualizing the change in the functional groups in the product. To this end, a database of the ranges assigned for the chemical shifts of ^{13}C NMR for the waxy products of the fuel obtained in the laboratory-scale catalytic pyrolysis unit is detailed (Ben and Ragauskas, 2011). Once received, the samples were stored refrigerated at 5 °C, in the absence of light, until analysis. Samples M1, M3, M5 presented solid residues. The analysis of these samples was carried out on the supernatant. All samples were characterized using a Bruker brand FURIER 300HD 300 MHz spectrometer. 50 mg of samples were weighed and dissolved in 1.5 mL of dimethyl sulfoxide (DMSO-d6). The experiments were 13C NMR. The number of sweeps was 1024, with a pulse delay of 5 s. The analyzes were carried out at room temperature. The spectral signals were adjusted with the solvent signal (39.52 ppm.) The processing of the spectra was carried out using the TopSpin 3.2 software from Bruker. Table 7 shows the database of chemical shifts. (Lab of Faculty of Science Report, Valparaiso, Chile; January 24, 2024).

In these spectra (Fig. 9a, M5, and Fig. 9b, M6) a shift of the peaks obtained and a change in their intensity can be observed, where the influence of the zeolite catalyst and the variation in temperature in the oil can be identified crude oil after the fast catalytic pyrolysis finished.

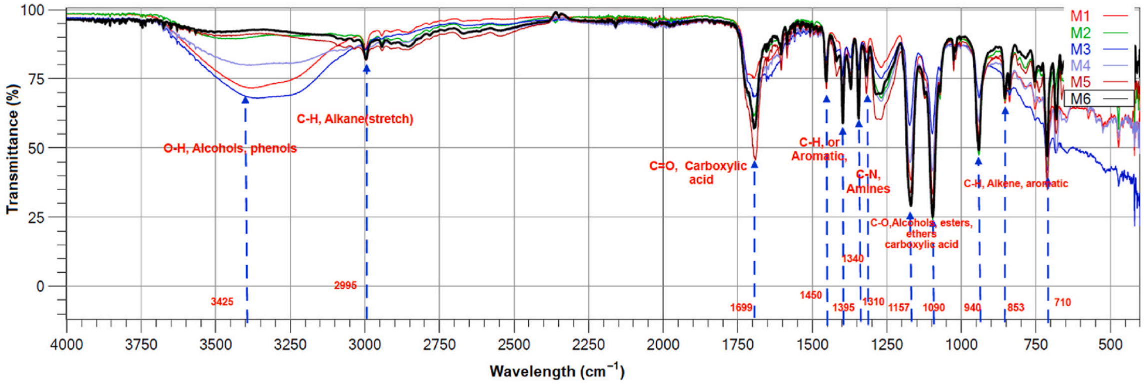

Fig. 8. Fourier transform infrared spectroscopy (FTIR) spectra of crude oil (waxy product) from 380 °C to 480 °C, with and without zeolite catalyst.

Table 7
Assignment of ^{13}C NMR chemical shifts and functional group distributions of the waxy product obtained in the PET pyrolysis unit (Ben and Ragauskas, 2011).

Functional Group	Integration Region (ppm)
Carbonyl or carboxyl bond	215.0–166.5
Aromatic C–O bond	166.5–142.0
Aromatic C–C bond	142.0–125.0
Aromatic C–H bond	125.0–95.8
Aliphatic C–O bond	95.8–60.8
Methoxyl-aromatic bond	60.8–55.2
Aliphatic C–C bond general	55.2–0.0

Fig. 10a M6 jointly shows the effect of the amount of zeolite catalyst and temperature, where it can be seen that there is a decrease (4.4 %) in the production of carbonyl groups when the temperature decreases (M6) when the temperature is lower and There is an absence of zeolite, while for sample M4 it increases (7.1 %) when feeding 100 g of the zeolite, so the use of the zeolite improves the rapid catalytic pyrolysis process. On the other hand, an increase in temperature (480 °C) and the weight of the zeolite (200 g) does not produce an improvement in the production of carbonyl groups, as shown with sample M5, where 6 % lower than sample M4 was obtained. Likewise, it has been observed that the presence of C–C aromatic bonds increases up to 73.31 % in the case of sample M4, in which 100 g of zeolite was fed at a temperature of 430 °C, but an increase in the amount of zeolite up to 200 g (M2) produces a decrease in the obtaining of these bonds, reaching 46.2 %, which is similar to the results with samples M3 of 47.7 % (without catalyst and 480 °C) and M6, 48.2 % (without catalyst and temperature of 380 °C). An increase in the temperature of the pyrolysis process to 480 °C in M5 allowed obtaining 58.7 % C–C aromatic bonds, which is lower than that obtained for sample M4. In Fig. 10a and Table 8 show this trend. According to the results obtained, the use of zeolite together with an increase in temperature will allow obtaining a greater amount of benzene and benzene derivatives, which agrees with what was found by Jia et al. (2020), and Du et al. (2016). This is because zeolite favors the anchoring of ether bonds in the process and later promotes the pyrolysis of most oxygenated compounds. On the other hand, the increase in temperature also favors the formation of the products, as can be observed in the case of samples M1 and M4, where the temperature increased from 380 °C to 430 °C maintaining the mass of the zeolite, and the same effect was observed for samples M2 and M5, where the increase in temperature from 380 °C to 430 °C improves the performance by 13.4 %. On the other hand, the C–C aliphatic bonds decreased from 24.6 % in M2 (catalyst 200 g and 430 °C) to 19 % in M5 (catalyst 200 g and 480 °C), that is, there was a decrease of 29.47 %. This finding coincides with those of Al-Asadi and Miskolczi (2018), and Jia et al. (2020), that is, an increase in the catalyst from 12.5 % to 25 % and the increase in temperature has an adverse effect. Fig. 9 shows the trends described in the spectra of the functional groups found by ^{13}C NMR analysis in each of the six samples processed in the pyrolysis unit at different temperature conditions and concentration of zeolite catalyst, and Fig. 10b shows Integration of the results of the crude oil obtained from pyrolysis of PET flake waste, only the results for the vibrations of aromatic compounds with C–C aromatic bonds, according to Table 8.

3.6. *CHEMCAD simulation results of fast catalytic pyrolysis*

For the pyrolysis simulation a simplified process flow diagram was constructed, including stoichiometric reactor, component separator, heat exchanger (condenser) and flash tank. Prior to the laboratory experiments, the real composition of the pyrolysis products was not known, so based on the literature review (Yoshioka et al., 2004), the most likely substances were considered: benzene, toluene, *p*-xylene, benzoic acid, bis(1-ethylhexyl) terephthalate (BEHP), light hydrocarbons (C1 – C4), carbon dioxide, carbon monoxide, carbon (solid residue) and nitrogen gas as inert atmosphere. It is important to point out, that in CHEMCAD simulations the stoichiometry must be accurate to at least six significant figures, otherwise the program will report a mass balance error. The most likely aromatic oxygenated compounds, like benzoic acid and BEHP, must be included in the mass balance, otherwise the stoichiometry will shift towards carbon dioxide and monoxide. Simulations were run at 380 °C, 430 °C and 480 °C, with only minor variations in the stoichiometry. The process flow diagram with temperature, pressure, and mass flowrate information of the 430 °C simulation is shown in Fig. 11 below; in this diagram, equipment No. 2 is not an actual piece of equipment, but only a component separator to simulate the solid residue (char) left in the reactor. As an example of the results at 430 °C, compositions of the gas effluent from the reactor, stream No. 5, and the crude fuel oil (liquid stream from the condenser), stream No. 8, are given in Tables 9 and 10 respectively. From the two aromatic oxygenated products of the pyrolysis reaction, BEHP doesn't appear to be formed at all.

An overall mass balance of the 430 °C simulation is summarized in Table 11 and represented as Sankey diagram in Fig. 12. The mass flowrates were scaled up from the laboratory tests by a factor of ten, and there was no significant difference between the results of the three cases and the test run.

The heat duty in the reactor appears in all cases as negative, which is to be explained by the high proportion of carbon dioxide and monoxide in the gases calculated by the stoichiometric reactor. Certainly, a better approach for the simulation can be achieved after considering the real analysis of the reaction products. As an example of the energy balance, the 430 °C simulation is shown in Table 12 below. The negative values are mainly due to the standard heat of formation and heat of reaction of the substances. These can be converted to positive values by changing the enthalpy reference state.

According to the results obtained, it is evident that the two variables

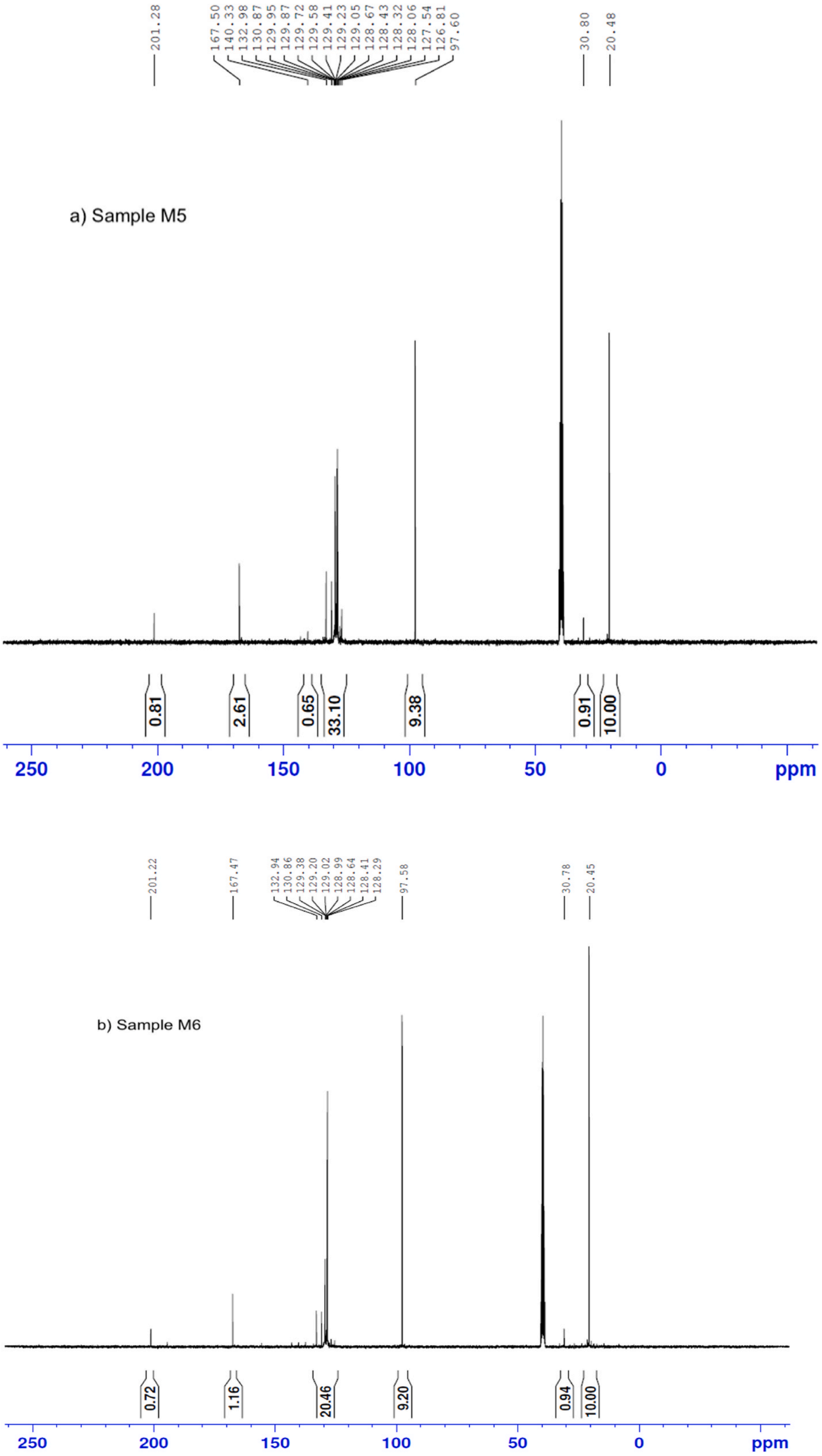

Fig. 9. ^{13}C NMR spectra of two crude oil samples obtained from the pyrolysis of PET flake waste with and without catalyst, 800 g samples for 60 min at 480 °C (a) and 380 °C (b).

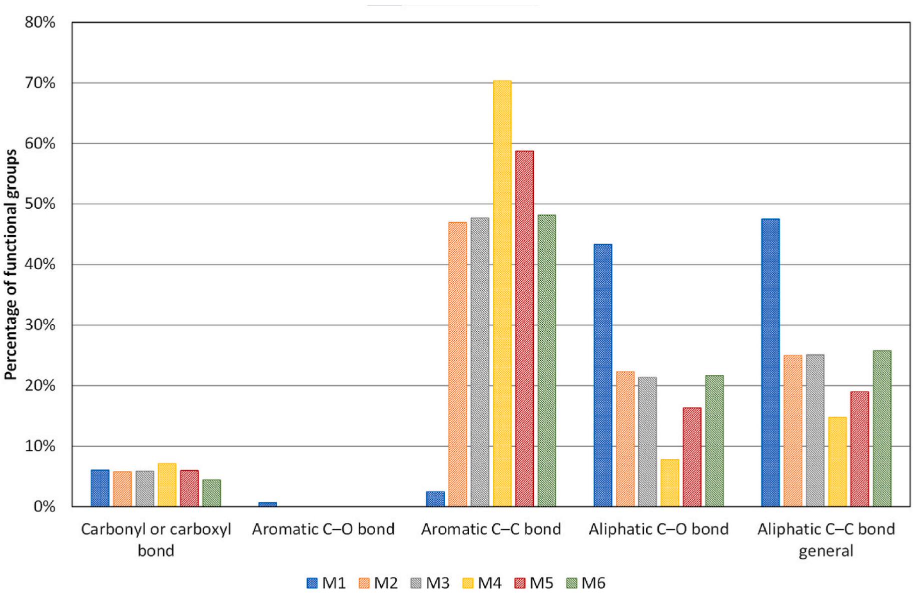

Fig. 10a. Integration of the results of the waxy products obtained from the pyrolysis of waste PET flake. The products are presented in relation to the carbon percentage.

Table 8
Results obtained in C–C aromatic bonds in the pyrolysis of PET flakes.

Sample	Catalyst, g	Temperature, °C	Aromatic C–C bond
M1	100	380	35.3
M6	0	380	20.4
M2	200	430	46.2
M4	100	430	73.3
M3	0	480	47.7
M5	200	480	33.7

studied (catalyst and temperature) influence the performance and composition of the crude oil; firstly the weight of the zeolite catalyst with respect to the weight of the PET waste, and to a lesser extent the variation in temperature; That is to say, with 12.5 % of zeolite catalyst with respect to the weight of PET waste (100 g of catalyst/800 g of PET waste), the best quality crude oil yield is obtained (20 %). It was observed that when feeding 100 g of zeolite catalyst on the bed of PET waste, it covers about 5 mm. thick inside the reactor, and when the pyrolysis gases are generated 40 min into the process, there is good contact of the pyrolysis gases with the catalyst, which facilitates the reduction of the activation energy of the endothermic decomposition reaction of PET waste. This result is consistent with the findings of Jia et al. (2020), who obtained 21 % crude oil at 450 °C but with a catalyst ratio of 2–4 with respect to the sample; On the other hand, Sivagami et al. (2022) obtained a lower yield (10 % crude oil) but at temperatures between 450 °C and 500 °C. Regarding temperature, it was determined that it has less influence than the catalyst; It was verified that at the temperature of 430 °C (M4, 12.5 % of catalyst is used), a better yield of crude oil was obtained in terms of quality (20 %) and 73.3 % of C-C

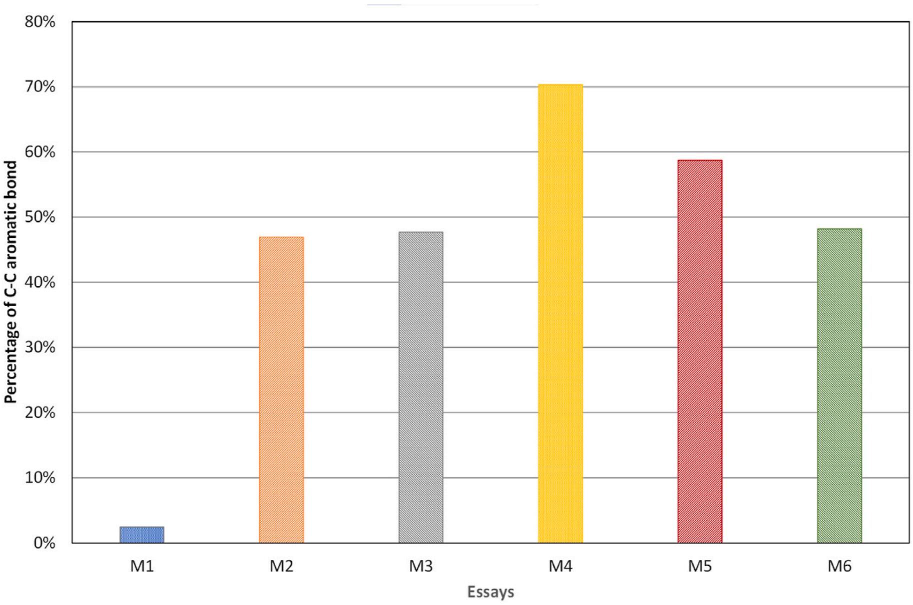

Fig. 10b. Integration of the results of the crude oil obtained from pyrolysis of PET flake waste. Only the results for the vibrations of aromatic compounds with C–C aromatic bonds, according to Table 8.

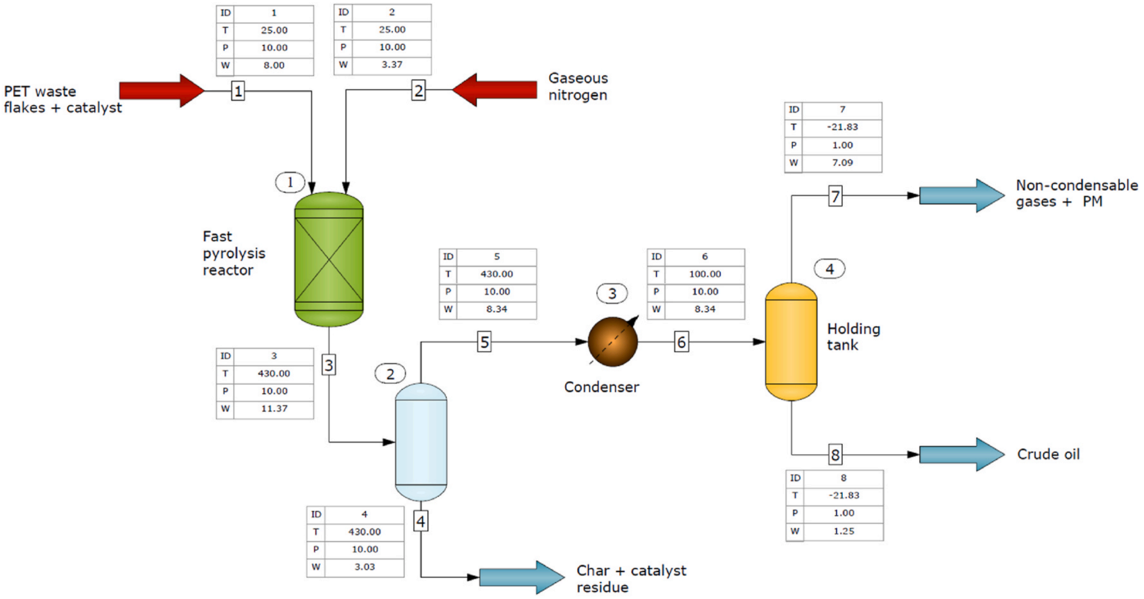

Fig. 11. CHEMCAD process flow diagram for the simulation of PET pyrolysis. Note: The boxes show temperatures in °C, pressure in bars, and mass flowrate in kg/h.

aromatic bonds compared to M3 where no catalyst is used (55 % C–C aromatic bonds) and 68 % crude oil but of poor quality; These findings are consistent with Jia et al. (2020), who at a temperature of 600 °C obtain a yield of 69 % of crude oil also without the use of catalyst. It is suggested to evaluate mixtures of PET with other plastics such as polypropylene, HDPE, LDPE, to find the best performance of the pyrolysis process through Machine Learning. The obtained crude oil could be refined and its performance in engines be evaluated by making mixtures with other fuels. This would allow waste plastics to have potential value, closing the circuit of the circular economy.

Table 9
Molar composition of the gas effluent from the reactor.

Component	Molar composition (%)
Benzene	0.31
Toluene	0.03
p-Xylene	0.01
Benzoic acid	0.00
BEHP	0.00
Methane	0.76
Ethane	3.45
Propane	3.09
Butane	2.56
Carbon dioxide	14.42
Carbon monoxide	21.46
Nitrogen	53.89

Table 10
Mass composition of the crude oil.

Component	Mass composition (%)
Benzene	20.23
Toluene	9.91
p-Xylene	7.85
Benzoic acid	60.34
BEHP	0.00
Methane	0.00
Ethane	0.04
Propane	0.23
Butane	1.07
Carbon dioxide	0.00
Carbon monoxide	0.00
Nitrogen	0.00

Table 11
Overall mass balance of the 430 °C simulation.

Inputs (kg/h)		Outputs (kg/h)	
PET waste	6.0000	Char + catalyst residue	3.0320
Catalyst	2.0000	Non-cond. gases	7.0935
Nitrogen	3.3730	Crude oil	1.2475
Total	11.3730	Total	11.3730

4. Conclusions

The rapid catalytic pyrolysis of PET flake waste with a constant sample of 800 g of PET was carried out in a fixed bed reactor, using activated zeolite as a catalyst with different doses (0 %, 12.5 % and 25 %) and different temperatures (380 °C, 430 °C and 480 °C), in an inert atmosphere with a flowrate of gaseous nitrogen of 4.5 L/min. After the tests were conducted in the catalytic pyrolysis unit, it was seen that the percentage of zeolite catalyst and the temperature variation have a greater influence on the yield of the crude oil. The feeding of zeolite catalyst in a percentage of 12.5 % at a temperature of 430 °C, the pyrolysis process generates an increase in the production of crude oil and increases the generation of gases due to the breaking of the C–C bonds. The largest number of solid particles was generated at 380 °C without catalyst, with a total of 11 %. As for the pyrolysis carbon residue, 14 % was generated (380 °C, catalyst 12.5 %). The highest generation of non-condensable gases was 71 % at 430 °C and 25 % catalyst, because the higher concentration of catalyst eases the breaking of C–C bonds.

On the other hand, it was observed that the beginning of pyrolysis gas generation is at 350 °C, which happens on average after 40 min; the maximum pressure of 1.21 MPa is reached after 50 min, and it is at that moment when the largest amount of crude oil is generated. The heating temperature and pressure in the reactor are closely related, the correlation coefficient, Pearson, and determination are 0.8998, 0.8883 and 0.8096, respectively, which show a positive correlation between the independent variable (temperature) and the dependent variable (pressure) in the pyrolysis reactor. The analyses of the ^{13}C NMR spectra for the crude oil show that with a concentration of 12.5 % of zeolite catalyst and a temperature of 430 °C, a better yield of crude oil is obtained, which is shown by the C–C aromatic bonds with a concentration of 70.3

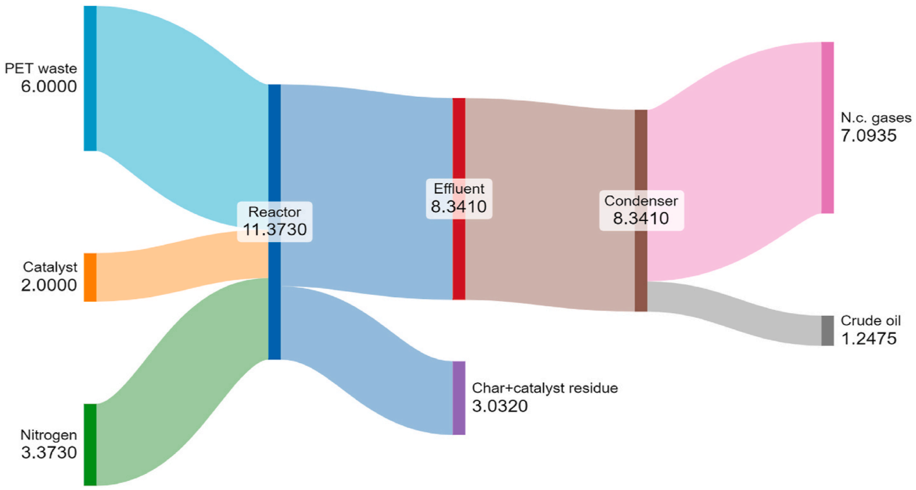

Fig. 12. Sankey diagram of mass balance in kg/h for the 430 °C simulation.

Table 12
Overall energy balance of the three simulations.

Inputs (MJ/h)		Outputs (MJ/h)	
Feed streams	−73.2049	Product streams	−94.2105
Total heating	0.0736	Total cooling	21.0792
Power added	0.0000	Power generated	0.0000
Total	−73.1313	Total	−73.1313

%. and in C–C aliphatic bonds with a concentration of 25.8 % in the product. Regarding the fugitive gas emissions that are generated during the cooling period of the pyrolysis unit, these are collected by the ventilation system and treated by adsorption and then the gases are released into the environment.

CRediT authorship contribution statement

E. Avalos-Ortecho: Writing – review & editing, Writing – original draft, Visualization, Validation, Supervision, Resources, Project administration, Methodology, Investigation, Funding acquisition, Formal analysis, Data curation, Conceptualization. **G. Power-Porto:** Writing – review & editing, Writing – original draft, Visualization, Software, Investigation, Formal analysis, Conceptualization. **S. Ponce Alvarez:** Methodology, Investigation, Formal analysis, Data curation, Conceptualization. **M. Gelmi-Candusso:** Writing – review & editing, Validation, Resources, Conceptualization. **C. Pardo-Martinez:** Writing – review & editing, Data curation, Conceptualization. **G. Concha-Oblitas:** Writing – original draft, Methodology, Investigation, Formal analysis.

Ethics

Authors should address any ethical issues that may arise after the publication of this manuscript.

Funding information

This research has been funded by Instituto de Investigación Científica (IDIC), Universidad de Lima, Perú. This project was the winner of one of the places in the IDIC 2022 research competition of the University of Lima. The allocation of financing resources and contractual conditions are registered in contract No. 2022 0151 01 signed by the authors of this research and the Universidad de Lima Rector's, on August 1, 2022.

Declaration of competing interest

The authors declare the following financial interests/personal relationships which may be considered as potential competing interests: Edilberto Avalos-Ortecho reports financial support was provided by University of Lima. There in not conflict of interest. If there are other authors, they declare that they have no known competing financial interests or personal relationships that could have appeared to influence the work reported in this paper.

Acknowledgments

The authors are grateful to the financial support from Instituto de Investigación Científica (IDIC) Universidad de Lima, Perú. We are also incredibly grateful to Ing. Ruben Torres for the excellent technical support during the conditioning, operation and development of the pyrolysis unit tests.

Appendix. ASupplementary data

Supplementary data to this article can be found online at https://doi.org/10.1016/j.clet.2025.100928.

Data availability

Data will be made available on request.

References

Al-Asadi, M., Miskolczi, N., 2018. Pyrolysis of polyethylene terephthalate containing real waste plastics using Ni loaded zeolite catalysts. In: IOP Conference Series: Earth and Environmental Science, vol. 154. Institute of Physics Publishing.

Andersen, M., Sætre, K.A., Fredriksen, S., Pfeiffer, C., 2018. Simulation of the pyrolysis process: from plastic waste to environmentally friendly fuel. In: Proceedings of the 59th Conference on Simulation and Modeling (SIMS 59), 303–307, 26-28 September 2018, Oslo Metropolitan University, Norway, vol. 153. Linköping University Electronic Press.

Armenise, S., Wong, S.L., Ramírez-Velasquez, J.M., Launay, F., Wuebben, D., Ngadi, N., Rams, J., Muñoz, M., 2021. Plastic waste recycling via pyrolysis: a bibliometric survey and literature review. J. Anal. Appl. Pyrolysis 158. https://doi.org/10.1016/j.jaap.2021.105265.

Artetxe, M., Lopez, G., Amutio, M., Elordi, G., Olazar, M., Bilbao, J., 2010. Operating conditions for the pyrolysis of poly-(ethylene terephthalate) in a conical spouted-bed reactor. Ind. Eng. Chem. Res. 49 (5), 2064–2069. https://doi.org/10.1021/ie900557c.

Ben, H., Ragauskas, A.J., 2011. NMR characterization of pyrolysis oils from kraft lignin. https://doi.org/10.1021/ef2001162.

Blaine, R.L. n.d. Thermal Applications Note TN048. Polymer heats of fusion. https://www.tainstruments.com/pdf/literature/TN048.pdf.

Charlton-Howard, H.S., Bond, A.L., Rivers-Auty, J., Lavers, J.L., 2023. 'Plasticosis'—characterizing macro- and microplastic-associated fibrosis in seabird tissues. J. Hazard Mater. 1–11.

ChemBK, 2023. Poly(ethylene terephthalate). https://www.chembk.com/en/chem/pet.

Çit, I., Sinag, A., Yumak, T.Y., Uçar, S., Misirlioğlu, Z., Cannel, M., 2010. Comparative pyrolysis of polyolefins (PP and LDPE) and PET. Polym. Bull. 64 (8), 817–834. https://doi.org/10.1007/s00289-009-0225-x.

Daniel, C., 1959. Use of half-normal plots in interpreting factorial two-level experiments. Technometrics 1 (4), 311–341.

Dhahak, A., Hild, G., Rouaud, M., Mauviel, G., Burkle-Vitzthum, V., 2019. Slow pyrolysis of polyethylene terephthalate: online monitoring of gas production and quantitative analysis of waxy products. J. Anal. Appl. Pyrolysis 142. https://doi.org/10.1016/j.jaap.2019.104664.

Diaz- Silvarrey, L.S., McMahon, A., Phan, A.N., 2018. Benzoic acid recovery via waste poly(ethylene terephthalate) (PET) catalytic pyrolysis using sulphated zirconia catalyst. J. Anal. Appl. Pyrolysis 134, 621–631. https://doi.org/10.1016/j.jaap.2018.08.014.

Du, S., Valla, J.A., Parnas, R.S., Bollas, G.M., 2016. Conversion of polyethylene terephthalate based waste carpet to benzene-rich oils through thermal, catalytic, and catalytic steam pyrolysis. ACS Sustain. Chem. Eng. 4 (5), 2852–2860. https://doi.org/10.1021/acssuschemeng.6b00450.

Eimontas, J., Striūgas, N., Abdelnaby, M.A., Yousef, S., 2021. Catalytic pyrolysis kinetic behavior and TG-FTIR-GC–MS analysis of metallized food packaging plastics with different concentrations of ZSM-5 zeolite catalyst. Polymers 13 (5), 1–15. https://doi.org/10.3390/polym13050702.

Erkmen, B., Ozdogan, A., Ezdesir, A., Celik, G., 2023. Can pyrolysis oil Be used as a feedstock to close the gap in the circular economy of polyolefins? Polymers 15 (4). https://doi.org/10.3390/polym15040859.

Farah, S., Kunduru, K.R., Basu, A., Domb, A.J., 2015. Molecular weight determination of polyethylene terephthalate. In: Visakh, P.M., Liang, M. (Eds.), Poly(Ethylene Terephthalate)-Based Blends, Composites and Nanocomposites, vol. 8. Elsevier Inc, pp. 143–165.

Fulgencio-Medrano, L., García-Fernández, S., Asueta, A., Lopez-Urionabarrenechea, A., Perez-Martinez, B.B., Arandes, J.M., 2022. Oil production by pyrolysis of real plastic waste. Polymers 14 (3), 553. https://doi.org/10.3390/polym14030553.

Geissdoerfer, M., Savaget, P., Bocken, N.M.P., Hultink, E.J., 2017. The circular economy–A new sustainability paradigm. J. Clean. Prod. (143), 757–768.

Ghosh, T., Avery, G., Bhatt, A., Uekert, T., Walzberg, J., Carpenter, A., 2023. Towards a circular economy for PET bottle resin using a system dynamics inspired material flow model. J. Clean. Prod. 383. https://doi.org/10.1016/j.jclepro.2022.135208.

Gracida-Alvarez, U.R., Xu, H., Benavides, P.T., Wang, M., Hawkins, T.R., 2023. Circular economy sustainability analysis framework for plastics: application for poly (ethylene terephthalate) (PET). ACS Sustain. Chem. Eng. 11 (2), 514–524. https://doi.org/10.1021/acssuschemeng.2c04626.

Grause, G., Handa, T., Kameda, T., Mizoguchi, T., Yoshioka, T., 2011. Effect of temperature management on the hydrolytic degradation of PET in a calcium oxide filled tube reactor. Chem. Eng. J. 166 (2), 523–528. https://doi.org/10.1016/j.cej.2010.11.010.

Gu, H., AlFayez, F., Ahmed, T., Bashir, Z., 2019. Poly(ethylene terephthalate) powder—a versatile material for additive manufacturing. Polymers 11 (2), 2041. https://doi.org/10.3390/polym11122041.

Hossain, R., Islam, M.D., Ghose, A., Sahajwalla, V., 2022. Full circle: challenges and prospects for plastic waste management in Australia to achieve circular economy. J. Clean. Prod. (368).

James, C., Armstrong, M., Washington, G., Biaglow, A., 2020. Consistency of thermodynamic properties from CHEMCAD process simulations. Chem. Data Collect. 27. https://doi.org/10.1016/j.cdc.2020.100371.

Jensen, N., 1956. Vapor pressure of plastic materials. J. Appl. Phys. 27, 1460. https://doi.org/10.1063/1.1722289.

Jia, H., Haoxi, B., Ying, L., Wang, R., 2020. Catalytic fast pyrolysis of poly(ethylene terephthalate) (PET) with zeolite and nickel chloride. Polymers 12 (3). https://doi.org/10.3390/polym12030705.

Kim, S.-S., Kim, S., 2004. Pyrolysis characteristics of polystyrene and polypropylene in a stirred batch reactor. Chem. Eng. J. 98 (1–2), 53–60. https://doi.org/10.1016/S1385-8947(03)00184-0.

Kosa, M., Ben, H., Theliander, H., Ragauskas, A.J., 2011. Pyrolysis oils from CO_2 precipitated kraft lignin. Green Chem. 13 (11), 3196–3202. https://doi.org/10.1039/c1gc15818j.

Krzywda, R., Wrzesińska, B., 2021. Simulation of the condensation and fractionation unit in waste plastics pyrolysis plant. Waste and Biomass Valoriz. 12 (1), 91–104. https://doi.org/10.1007/s12649-020-00994-7.

Kubowicz, S., Booth, A.M., 2017. Biodegradability of plastics: challenges and misconceptions. Environ. Sci. Technol. 51 (21), 12058–12060.

Kumagai, S., Hasegawa, I., Grause, G., Kameda, T., Yoshioka, T., 2015. Thermal decomposition of individual and mixed plastics in the presence of CaO or $Ca(OH)_2$. J. Anal. Appl. Pyrolysis 113, 584–590. https://doi.org/10.1016/j.jaap.2015.04.004.

LePree, J., 2015. Process simulation software chemical engineering. Chem. Eng. 25–29.

Lee, K.H., 2012. Effects of the types of zeolites on catalytic upgrading of pyrolysis wax oil. J. Anal. Appl. Pyrolysis 94, 209–214. https://doi.org/10.1016/j.jaap.2011.12.015.

Li, C., Ataei, F., Atashi, F., Hu, X., Gholizadeh, M., 2021. Catalytic pyrolysis of polyethylene terephthalate over zeolite catalyst: characteristics of coke and the products. Int. J. Energy Res. 45 (13), 19028–19042. https://doi.org/10.1002/er.7078.

Lombardo, G., Ebin, B., Steenari, B.M., Alemrajabi, M., Karlsson, I., Petranikova, M., 2021. Comparison of the effects of incineration, vacuum pyrolysis and dynamic pyrolysis on the composition of NMC-lithium battery cathode-material production scraps and separation of the current collector. Resour. Conserv. Recycl. 164. https://doi.org/10.1016/j.resconrec.2020.105142.

López, A., De Marco, I., Caballero, B.M., Laresgoiti, M.F., Adrados, A., 2011. Influence of time and temperature on pyrolysis of plastic wastes in a semi-batch reactor. Chem. Eng. J. 173 (1), 62–71. https://doi.org/10.1016/j.cej.2011.07.037.

Lyon, R.E., Hackett, S.M., Walters, R.N., 1998. Heats of combustion of high-temperature polymers. DOT/FAA/AR-TN97/8. https://www.fire.tc.faa.gov/pdf/tn97-8.pdf.

Maafa, I.M., 2021. Pyrolysis of polystyrene waste: a review. Polymers 13 (2), 1–30.

Mabitsela, L., Telukdarie, A., Munsamy, M., 2022. Modeling for cleaner production & optimization. Procedia Comput. Sci. 217, 679–688. https://doi.org/10.1016/j.procs.2022.12.264.

MatWeb Material Property Data, 2023. Overview of Materials for Polyethylene Terephthalate (PET). Unreinforced. https://www.matweb.com/search/DataSheet.aspx?MatGUID=a696bdcdff6f41dd98f8eec3599eaa20&ckck=1.

Miandad, R., Rehan, M., Barakat, M.A., Aburiazaiza, A.S., Khan, H., Ismail, I.M.I., Dhavamani, J., Gardy, J., Hassanpour, A., Nizami, A.S., 2019. Catalytic pyrolysis of plastic waste: moving toward pyrolysis based biorefineries. Front. Energy Res. 7. https://doi.org/10.3389/fenrg.2019.00027.

Montgomery, D.C., 2017. Design and Analysis of Experiments, ninth ed. Wiley, p. 254. Ch. 6.

Moya, D., Aldás, C., López, G., Kaparaju, P., 2017. Municipal solid waste as a valuable renewable energy resource: a worldwide opportunity of energy recovery by using waste-to-energy technologies. Energy Proc. 134, 286–295. Elsevier Ltd.

Muneer, B., Zeeshan, M., Qaisar, S., Razzaq, M., Iftikhar, H., 2019. Influence of in-situ and ex-situ HZSM-5 catalyst on Co-pyrolysis of corn stalk and polystyrene with a focus on liquid yield and quality. J. Clean. Prod. 237. https://doi.org/10.1016/j.jclepro.2019.117762.

Nait-Ali, L.K., Colin, X., Bergeret, A., 2011. Kinetic analysis and modeling of PET macromolecular changes during its mechanical recycling by extrusion. Polym. Degrad. Stabil. 96 (2), 236–246. https://doi.org/10.1016/j.polymdegradstab.2010.11.004.

Olcese, R., Carré, V., Aubriet, F., & Dufour, A. n.d. Selectivity of Bio-Oils Catalytic Hydrotreatment Assessed by Petroleomic and GC*GC/MS-FID Analysis Supporting Information.

Padmanabhan, S., Giridharan, K., Stalin, B., Kumaran, S., Kavimani, V., Nagaprasad, N., Jule, L.T., Krishnaraj, R., 2022. Energy recovery of waste plastics into diesel fuel with ethanol and ethoxy ethyl acetate additives on circular economy strategy. Sci. Rep. 12 (1). https://doi.org/10.1038/s41598-022-09148-2.

Papari, S., Bamdad, H., Berruti, F., 2021. Pyrolytic conversion of plastic waste to value-added products and fuels: a review. Materials 14, 2586. https://doi.org/10.3390/ma14102586.

Papuga, S., Djurdjevic, M., Ciccioli, A., Vecchio Ciprioti, S., 2022. Catalytic pyrolysis of plastic waste and molecular symmetry effects: a review. Symmetry 15 (1), 38. https://doi.org/10.3390/sym15010038.

Plastics Europe, 2023. Plastics – the fast facts 2023. Plast Eur. 1–4. https://plasticseurope.org/knowledge-hub/plastics-the-fast-facts-2023/.

Polymer Database, 2023. Polyethylene Terephthalate.

Potnuri, R., Suriapparao, D.V., Rao, C.S., Kumar, T.H., 2022. Understanding the role of modeling and simulation in pyrolysis of biomass and waste plastics: a review. In: Bioresource Technology Report, vol. 20.

Ramos, T., Christensen, T.B., Oturai, N., Syberg, K., 2023. Reducing plastic in the operating theatre: towards a more circular economy for medical products and packaging. J. Clean. Prod. 383. https://doi.org/10.1016/j.jclepro.2022.135379.

Rosenberg, M., Budde Christensen, T., Ramos, T.M., Syberg, K., 2021. A review of the plastic value chain from a circular economy perspective. J. Environ. Manag. 302, 1–9.

Setaram KEP Technologies, 2020. Determination of Crystallinity of PET by DSC. https://setaramsolutions.com/app/uploads/sites/2/2020/09/ANS-002-Determination-of-cristallinity-of-PET-by-DSC.pdf.

Sharuddin, S.D.A., Abnisa, F., Daud, W.M.A.W., Wan, D., Aroua, M.K., 2017. Energy recovery from pyrolysis of plastic waste: study on non-recycled plastics (NRP) data as the real measurement of plastic waste. Energy Convers. Manag. 148, 925–934. https://doi.org/10.1016/j.enconman.2017.06.046.

Singh, E., Mishra, R., Kumar, A., Kumar Shukla, S., Shang, L.L., Kumar, S., 2022. Circular economy-based environmental management using biochar: driving towards sustainability. Process Saf. Environ. Prot. 163, 585–600.

Sivagami, K., Kumar, K.V., Tamizhdurai, P., Govindarajan, D., Kumar, M., Nambi, I., 2022. Conversion of plastic waste into fuel oil using zeolite catalysts in a bench-scale pyrolysis reactor. RSC Adv. 12 (13), 7612–7620. https://doi.org/10.1039/d1ra08673a.

The Engineering Toolbox, 2023. Polymers – specific Heats. Specific heat of polymers like epoxy. PET, polycarbonate and more. https://www.engineeringtoolbox.com/specific-heat-polymers-d_1862.html.

The Polymer Design Team, 2016. Polymer Design: PET Chemical Recycling—Preliminary Process Flow and Data Sets, p. 2016.

Vaishnavi, M., Vasanth, P.M., Rajkumar, S., Gopinath, K.P., Devarajan, Y., 2023. A critical review of the correlative effect of process parameters on pyrolysis of plastic wastes. J. Anal. Appl. Pyrolysis 170.

Venkatachalam, S., Nayak, S.G., Labde, J.V., Gharal, P.R., Rao, K., Kelkjar, A.K., 2012. Degradation and recyclability of poly(ethylene terephthalate). In: Saleh, H. (Ed.), Polyester, vol. 4. InTech Open. https://doi.org/10.5772/48612.

Wikipedia contributors, 2023. Polyethylene terephthalate. https://en.wikipedia.org/wiki/Polyethylene_terephthalate.

Yansaneh, O.Y., Zein, S.H., 2022. Latest advances in waste plastic pyrolytic catalysis. Processes 10 (4).

Yoshioka, T., Grause, G., Eger, C., Kaminsky, W., Okuwaki, A., 2004. Pyrolysis of poly (ethylene terephthalate) in a fluidised bed plant. Polym. Degrad. Stabil. (86), 499–504.

Zhang, Y., Ji, Y., Qian, H., 2021. Progress in thermodynamic simulation and system optimization of pyrolysis and gasification of biomass. Green Chem. Eng. 2 (3), 266–283.

Zhang, Y., Ji, G., Chen, C., Wang, Y., Wang, W., Li, A., 2020a. Liquid oils produced from pyrolysis of plastic wastes with heat carrier in rotary kiln. Fuel Process. Technol. 206, 106455.

Zhang, Y., Fu, Z., Wang, W., Ji, G., Zhao, M., Li, A., 2022. Kinetics, product evolution, and mechanism for the pyrolysis of typical plastic waste. ACS Sustain. Chem. Eng. 10 (1), 91–103.

Zhang, Y., Ji, G., Ma, D., Chen, C., Wang, Y., Wang, W., Li, A., 2020b. Exergy and energy analysis of pyrolysis of plastic wastes in rotary kiln with heat carrier. Process Saf. Environ. Prot. 142, 203–211.

Zhang, Y., Li, A., Zhang, Y.S., Xie, W., Liu, C., Peng, Y., Zhang, H., Kang, Y., Qu, B., Ji, G., 2024. In-situ catalytic pyrolysis of polyethylene to co-produce BTX aromatics and H_2 by Ni/ZSM-5 in the rotary reactor with solid heat carriers. Fuel 371 (Part A), 131950.